Xu et al., http://www.jcb.org/cgi/content/full/jcb.201008135/DC1



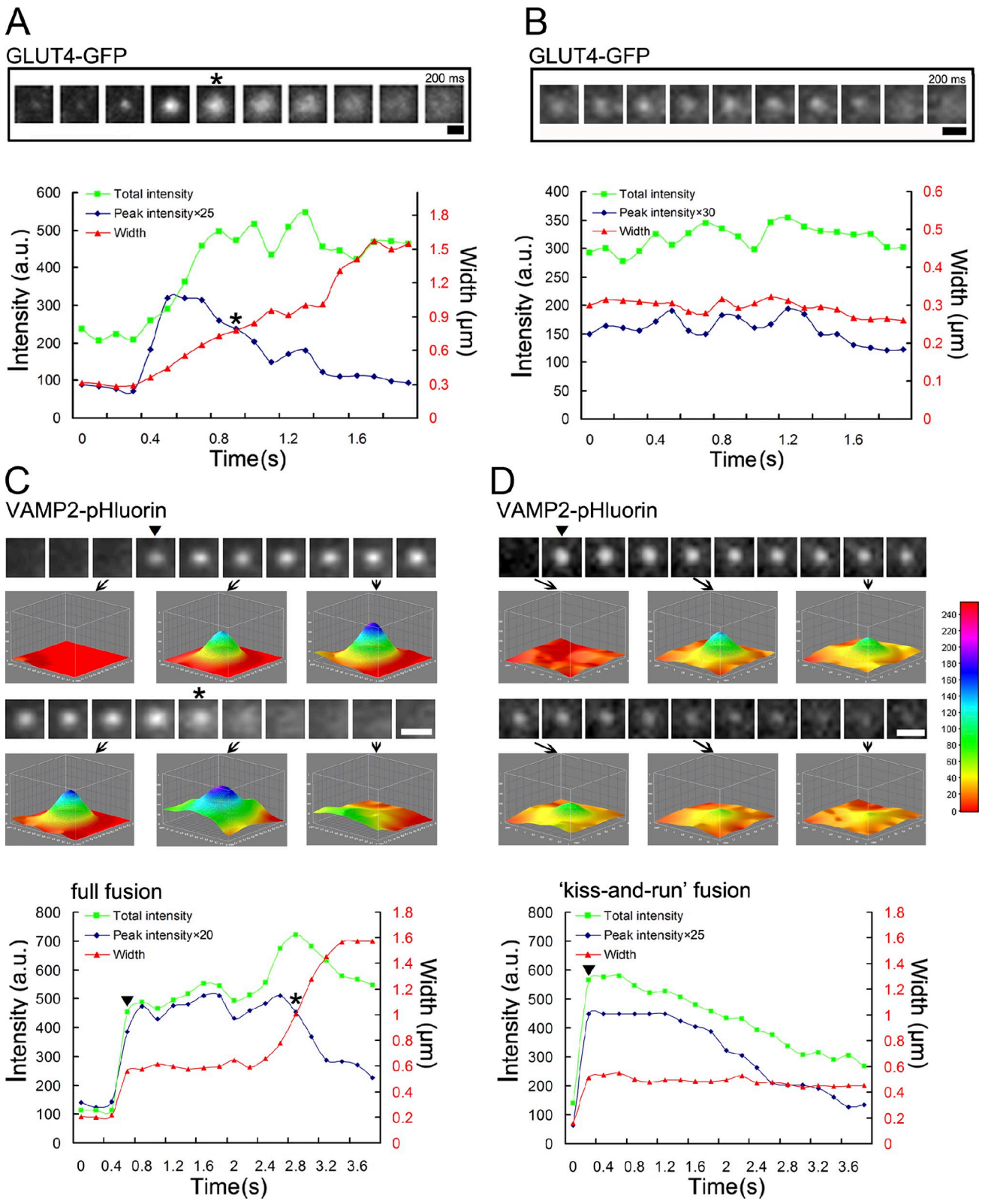


Figure S1. **Analysis of single vesicle fusion events.** (A) A GLUT4-GFP fusion event in a 3T3-L1 preadipocyte is shown (Fig. 1 C, example 1). A Gaussian fit was used to quantify the peak intensity, total intensity, and FWHM of the vesicle's fusion profile. (B) An example in a 3T3-L1 mature adipocyte, where a vesicle appeared but no fusion occurred (no increase in FWHM or peak intensity). (C and D) Examples of a VAMP2-pHluorin full fusion (C) and kiss-and-run (D) events in mature 3T3-L1 adipocytes. The 3D fusion profiles of selected frames (arrows) are shown with the peak intensity, total intensity, and FWHM plotted underneath. Note that the full vesicle fusion has an increase in the FWHM, whereas the kiss-and-run event does not (and in the latter, the slope of the peak intensity decay is shallower). Arrowheads indicate opening of the fusion pore; asterisks indicate full vesicle collapse. All intensities were normalized to their initial values. Interval: 200 ms. Bars, 1 μm.

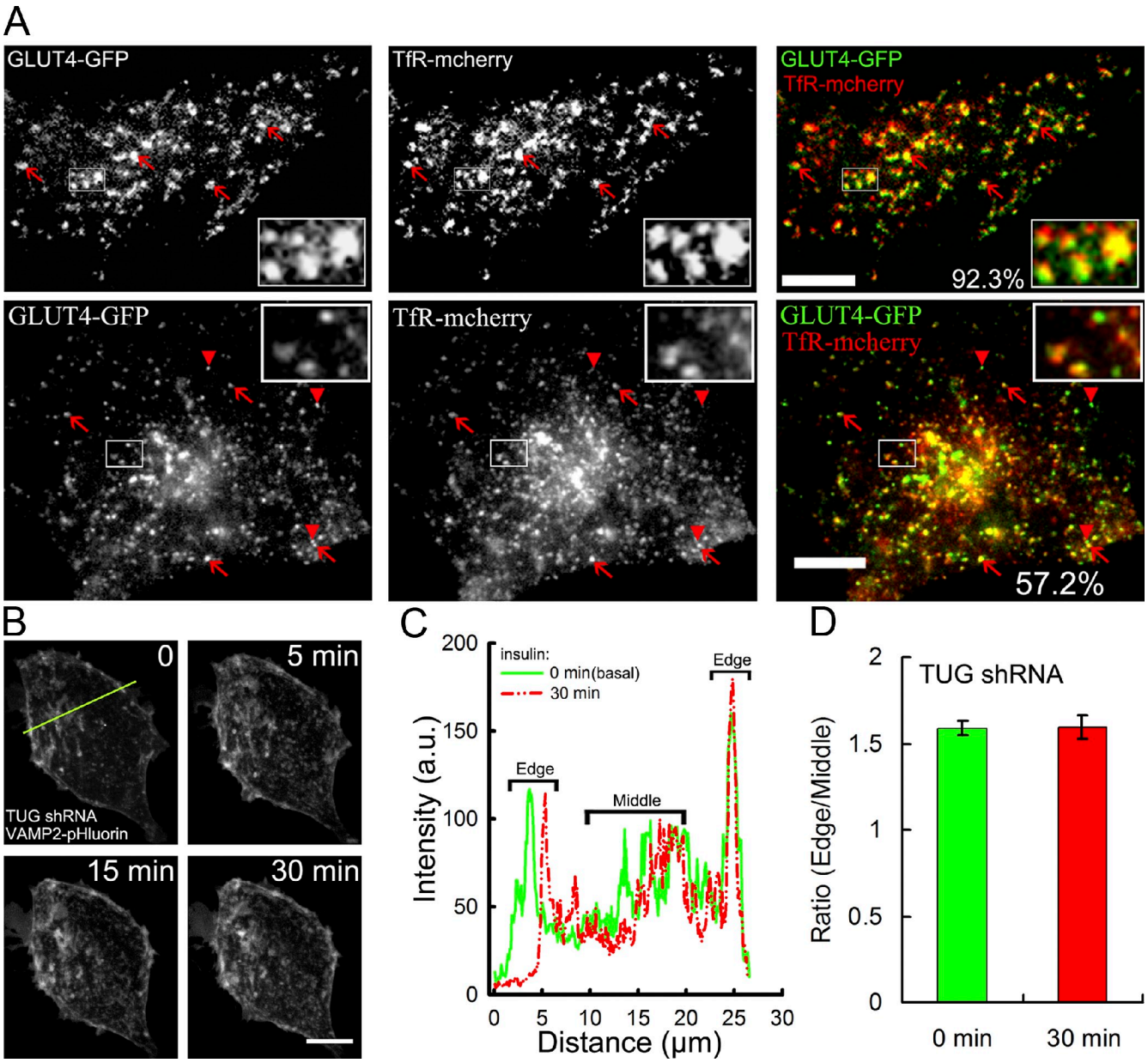


Figure S2. **Differentiation of 3T3-L1 adipocytes causes the targeting of GLUT4 to TfR-negative vesicles, and TUG shRNA disrupts VAMP2-pHluorin retention within unstimulated cells.** (A) Undifferentiated 3T3-L1 preadipocytes stably expressing GLUT4-GFP were transfected with a plasmid encoding TfR-mCherry (top). Mature 3T3-L1 adipocytes were electroporated with plasmids encoding GLUT4-GFP and TfR-mCherry (bottom). In both cases, cells were imaged by TIRFM. Colocalization of GLUT4 with TfR was 92.3 ± 2.6% in preadipocytes and 57.2 ± 4.8% in mature adipocytes (mean ± SEM by Pearson's coefficient). Arrows highlight colocalized compartments, whereas arrowheads show GLUT4-GFP that does not colocalize with TfR in mature adipocytes. Insets show enlarged views of the boxed areas. Bar, 10 μm. (B) 3T3-L1 adipocytes containing the TUG shRNA were electroporated with VAMP2-pHluorin and imaged by 3D time-lapse SDCM. Maximum z-projection images were taken before (0 min) and after (5–30 min) 100 nM insulin addition. (C) Fluorescence intensity line profiles (line in B) were plotted for images before (green) and 30 min after (red) insulin. (D) The ratio of edge-to-middle intensities from line profiles of five cells is plotted (error bars indicate mean ± SEM).

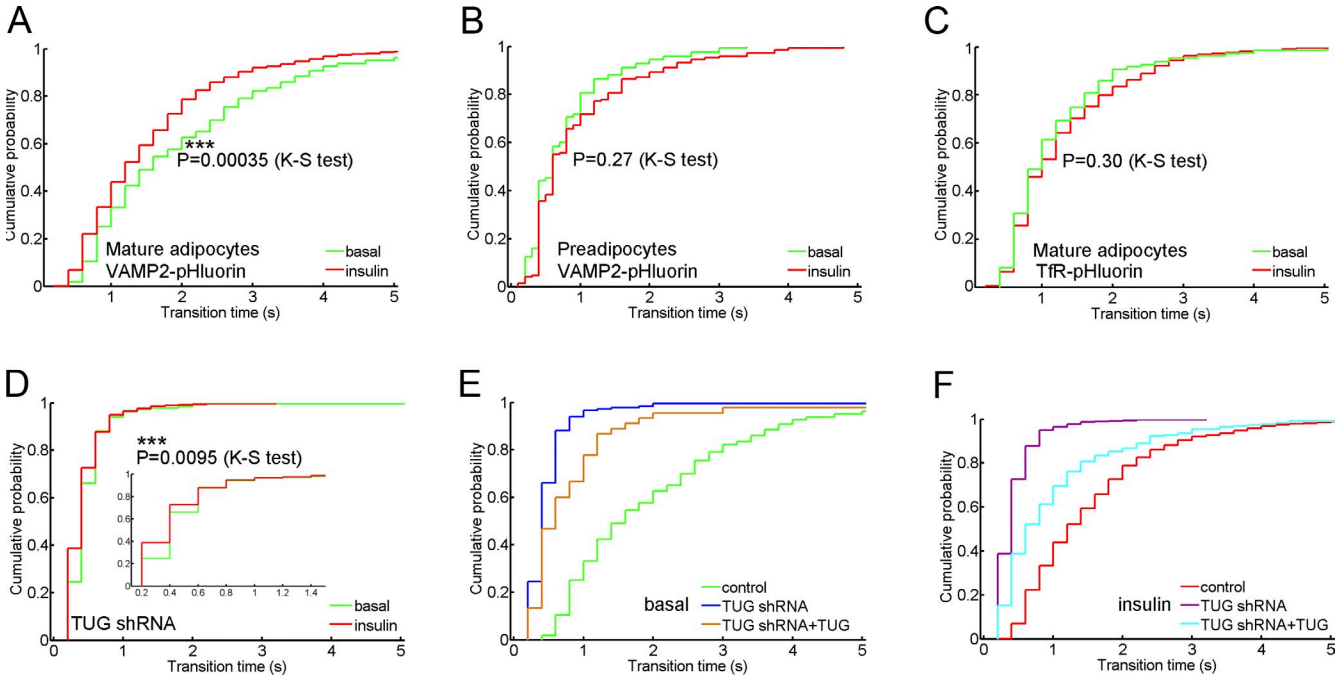


Figure S3. **Insulin regulates VAMP2-pHluorin fusion pore dynamics in mature 3T3-L1 adipocytes.** (A) Cumulative probability distributions of fusion pore transition times in basal and insulin-stimulated adipocytes. The transition time after insulin stimulation was significantly faster than in unstimulated cells (P = 0.00035, Kolmogorov-Smirnov [K-S] test), which indicates that insulin accelerates the fusion process. (B) Cumulative distributions of fusion pore transition times in basal and insulin-stimulated 3T3-L1 preadipocytes. (C) Cumulative distributions of fusion pore transition times measured using TfR-pHluorin in basal and insulin-stimulated 3T3-L1 adipocytes. (D) Cumulative distributions of fusion pore transition times in basal and insulin-stimulated adipocytes containing the TUG shRNA (P = 0.0095, K-S test), indicating that insulin accelerates fusion. (E and F) Cumulative distributions of fusion pore transition times in basal (E) and insulin-stimulated (F) 3T3-L1 adipocytes. Control, TUG shRNA, and rescued (TUG shRNA +TUG) cells are shown.

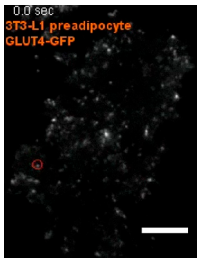


Video 1. **TIRFM imaging of exocytosis of GLUT4-GFP in a 3T3-L1 preadipocyte.** Frames were collected by TIRFM at 10 Hz and are shown at 30 frames per second. This video corresponds to the maximum projection image in Fig. 1 A and was highly compressed from the original 187 MB time-lapse movie. Red circles highlight fusion events, which are easily visualized. Bar, 10 µm.

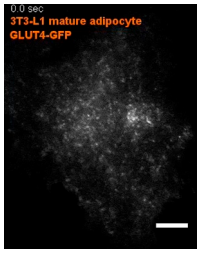


Video 2. **TIRFM of GLUT4-GFP in a mature insulin-stimulated 3T3-L1 adipocyte.** Frames were collected by TIRFM at 10 Hz and shown at 30 frames per second. This video corresponds to the maximum projection image in Fig. 1 B and was highly compressed from the original 387 MB time-lapse movie. Red circles highlight fusion events. Bar, 10 µm.

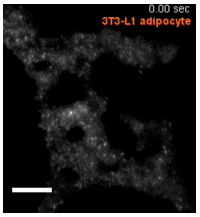


Video 3. **TIRFM of VAMP2-pHluorin translocation in a 3T3-L1 adipocyte.** Frames were collected by TIRFM at 5 Hz and are shown at 30 frames per second. This video corresponds to the cell in Fig. 4 C (control cell, at left). Red circles indicate the start of fusion (opening of the fusion pore), whereas green circles indicate the end of fusion. The video was highly compressed from the original 316 MB time-lapse movie. Note that the basal fusion rate is low, but is greatly augmented when insulin was added. Fusion events are easily detected by visual inspection. Bar, 10 μm.

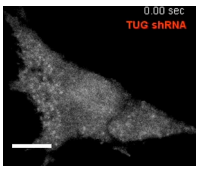


Video 4. **TIRFM of VAMP2-pHluorin in a 3T3-L1 adipocyte containing TUG shRNA.** Frames were collected by TIRFM at 5 Hz and are shown at 30 frames per second. This video corresponds to the cell in Fig. 4 C (TUG shRNA cell, at right). Red circles indicate the start of fusion (opening of the fusion pore), whereas green circles indicate the end of fusion. The video was highly compressed from the original 273 MB time-lapse movie. Note that the rate of fusion events rapidly increased ~20 s after insulin addition (~140 s). Bar, 10 μm.

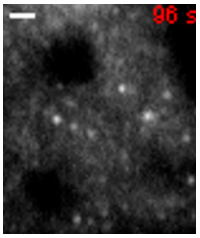


Video 5. **High-magnification cropped view of VAMP2-pHluorin exocytosis after insulin stimulation.** Frames were collected by TIRFM at 5 Hz and are shown at 5 frames per second. A region of interest was cropped from Video 3 without compression to better show full fusion events after insulin stimulation. Red circles indicate the start of fusion (opening of the fusion pore), whereas green circles indicate the end of fusion. Bar, 2 μm.